The Environment of "Mycobacterium avium subsp. hominissuis" Microaggregates Induces Synthesis of Small Proteins Associated with Efficient Infection of Respiratory Epithelial Cells

Citation	Babrak, L., Danelishvili, L., Rose, S. J., Kornberg, T., & Bermudez, L. E. (2015). The Environment of "Mycobacterium avium subsp. hominissuis" Microaggregates Induces Synthesis of Small Proteins Associated with Efficient Infection of Respiratory Epithelial Cells. Infection and Immunity, 83(2), 625-636. doi:10.1128/IAI.02699-14
DOI	10.1128/IAI.02699-14
Publisher	American Society for Microbiology
Version	Version of Record
Terms of Use	http://cdss.library.oregonstate.edu/sa-termsofuse

IAI Journals.ASM.org

The Environment of "*Mycobacterium avium* subsp. *hominissuis*" Microaggregates Induces Synthesis of Small Proteins Associated with Efficient Infection of Respiratory Epithelial Cells

Lmar Babrak,[a,b] Lia Danelishvili,[a] Sasha J. Rose,[a,b] Tiffany Kornberg,[a] Luiz E. Bermudez[a,b]

Department of Biomedical Sciences, College of Veterinary Medicine,[a] and Department of Microbiology, College of Science,[b] Oregon State University, Corvallis, Oregon, USA

"*Mycobacterium avium* subsp. *hominissuis*" is an opportunistic environmental pathogen that causes respiratory illness in immunocompromised patients, such as those with cystic fibrosis as well as other chronic respiratory diseases. Currently, there is no efficient approach to prevent or treat *M. avium* subsp. *hominissuis* infection in the lungs. During initial colonization of the airways, *M. avium* subsp. *hominissuis* forms microaggregates composed of 3 to 20 bacteria on human respiratory epithelial cells, which provides an environment for phenotypic changes leading to efficient mucosal invasion *in vitro* and *in vivo*. DNA microarray analysis was employed to identify genes associated with the microaggregate phenotype. The gene encoding microaggregate-binding protein 1 (MBP-1) (MAV_3013) is highly expressed during microaggregate formation. When expressed in noninvasive *Mycobacterium smegmatis*, MBP-1 increased the ability of the bacteria to bind to HEp-2 epithelial cells. Using anti-MBP-1 immune serum, microaggregate binding to HEp-2 cells was significantly reduced. By far-Western blotting, and verified by coimmunoprecipitation, we observed that MBP-1 interacts with the host cytoskeletal protein vimentin. As visualized by confocal microscopy, microaggregates, as well as MBP-1, induced vimentin polymerization at the site of bacterium-host cell contact. Binding of microaggregates to HEp-2 cells was inhibited by treatment with an antivimentin antibody, suggesting that MBP-1 expression is important for *M. avium* subsp. *hominissuis* adherence to the host cell. MBP-1 immune serum significantly inhibited *M. avium* subsp. *hominissuis* infection throughout the respiratory tracts of mice. This study characterizes a pathogenic mechanism utilized by *M. avium* subsp. *hominissuis* to bind and invade the host respiratory epithelium, suggesting new potential targets for the development of antivirulence therapy.

"*Mycobacterium avium* subsp. *hominissuis*" is an environmental bacterium ubiquitous in soil and natural water sources. In addition, *M. avium* subsp. *hominissuis* is an opportunistic pathogen that poses a major risk to immunocompromised patients, such as those with HIV infection, cystic fibrosis, and chronic respiratory diseases such as bronchiectasis and chronic obstructive pulmonary diseases (COPD). During the AIDS epidemic, mycobacterial infections became a widespread medical concern due to high morbidity and mortality in severely immunocompromised individuals (1). In recent years, there has been a significant increase in the incidence of nontuberculous mycobacterial (NTM) lung infections, including in cystic fibrosis patients, where *M. avium* subsp. *hominissuis* accounts for 72% of mycobacterial infections (2–4). Studies have also found an increase in NTM lung infections in middle-aged women with no known underlying conditions (5).

Due to the hardy cell wall of *M. avium* subsp. *hominissuis* and its natural resistance to many antibiotics, treatment is lengthy and encompasses a combination of various antibiotics, such as macrolides and ethambutol, with a potential decrease in patient compliance. In addition, *M. avium* subsp. *hominissuis* infection has a high incidence of reoccurrence and frequently results in antibiotic resistance over time, supporting experimental data that show that biofilm production in the lungs may play a role in the establishment of infection (6, 7). In fact, *M. avium* subsp. *hominissuis* biofilms are resistant to currently used antimycobacterial therapies, and studies suggest that biofilm production is closely associated with the ability to cause lung infections (7, 8).

Pathogenic microorganisms utilize a number of strategies to establish infection within the host. Respiratory pathogens are inhaled into the lungs and bind to and cross the respiratory mucosa, all while evading host defenses. The ability of bacteria to adhere to and invade the mucosal epithelium is often mediated by interaction with host proteins and modulation of host cell signaling. *Streptococcus pneumoniae* uses the surface-exposed bacterial protein PspC to facilitate adhesion to the host cell surface by interacting with vitronectin, a host glycoprotein (9). Several mycobacterial proteins that facilitate adhesion to the host epithelial cell membrane, such as fibronectin attachment proteins (FAP), histone-like protein (Hlp), the heparin-binding hemagglutinin (HBHA), and antigen 85, have been characterized (10–13). Pathogens also take advantage of surface-exposed cytoskeletal proteins for successful adhesion and invasion of epithelial cells. Dam et al.

Received 3 October 2014 **Returned for modification** 5 November 2014
Accepted 14 November 2014

Accepted manuscript posted online 24 November 2014

Citation Babrak L, Danelishvili L, Rose SJ, Kornberg T, Bermudez LE. 2015. The environment of "*Mycobacterium avium* subsp. *hominissuis*" microaggregates induces synthesis of small proteins associated with efficient infection of respiratory epithelial cells. Infect Immun 83:625–636. doi:10.1128/IAI.02699-14.

Editor: B. A. McCormick

Address correspondence to Luiz E. Bermudez, luiz.bermudez@oregonstate.edu.

Supplemental material for this article may be found at http://dx.doi.org/10.1128/IAI.02699-14.

doi:10.1128/IAI.02699-14

have shown that cytoskeletal rearrangement through activation of Cdc42 by the product of the mycobacterial *fadD2* gene results in actin polymerization, which is necessary for efficient invasion of intestinal mucosal epithelial cells (14). Other studies have observed that inhibition of actin polymerization by cytochalasin b prior to infection substantially decreases *M. avium* subsp. *hominissuis* epithelial cell invasion (14, 15). In addition, other cytoskeletal proteins, such as vimentin, a type III intermediate filament protein, are also used by both bacterial and viral pathogens as a receptor for adherence and invasion host cells. The *Escherichia coli* K1 virulence factor IbeA$^+$ was shown to directly bind to vimentin and was required for signaling and invasion of human brain microvascular cells (HBMEC) (16).

Bacterial aggregation has been shown to be important for the pathogenesis of infections caused by *Pseudomonas aeruginosa*, *Streptococcus pyogenes*, uropathogenic *Escherichia coli*, *Bordetella pertussis*, *Neisseria meningitidis*, and *Enterococcus* spp. (17–22). Microaggregate formation is often mediated by cell surface proteins, such as fimbriae and pili, and can have a protective effect in the presence of antibiotics, enhance bacterial adherence to host cells, and serve as a prelude to early biofilm formation (18, 20, 23). *N. meningitidis* expresses a type IV pilus (Tfp) that not only is involved in host cell adhesion, twitching motility, and DNA uptake but also mediates formation of bacterial aggregates, which have been shown to be necessary for efficient infection in mice (24).

Previous findings in our laboratory by Yamazaki et al. showed that exposure of *M. avium* subsp. *hominissuis* to bronchial cells for a period of 24 h resulted in the formation of microaggregates consisting of 3 to 20 bacteria (8). The microaggregates were shown to invade respiratory epithelial cells with greater efficiency than those bacteria that were not in microaggregates (planktonic bacteria), and this invasive phenotype was not induced by epithelial cell supernatant (8). Our working model postulates that during initial colonization of the airways, *M. avium* subsp. *hominissuis* forms microaggregates on the surfaces of airway epithelial cells, which provides an environment for phenotypic changes leading to efficient mucosal crossing.

In this study, we investigated a virulence strategy utilized by *M. avium* subsp. *hominissuis* during the early stages of respiratory infection. We have characterized microaggregate formation by utilizing DNA microarrays to obtain whole-genome transcriptional profiling of bacteria under the conditions of microaggregate formation and have identified a highly expressed gene encoding microaggregate-binding protein 1 (MBP-1) (MAV_3013), which is important for bacterial adhesion to the respiratory epithelium. Overall, our data provide insights into the initial interaction between *M. avium* subsp. *hominissuis* and the respiratory mucosa.

MATERIALS AND METHODS

Bacterial cultures. *Mycobacterium avium* strain 104 (serovar 1) was isolated from blood of AIDS patients. *M. avium* subsp. *hominissuis* strain 3388 (MAC3388), isolated from a human mycobacterial lung infection, was a gift from Barbara Brown-Elliot (Tyler, TX). *Mycobacterium smegmatis* mc^2 155 was kindly provided by W. Jacobs, Jr. (Albert Einstein School of Medicine, Bronx, NY). Mycobacterial strains were cultured on Middlebrook 7H10 agar supplemented with 10% oleic acid, albumin, dextrose, and catalase to log phase (Hardy Diagnostics, Santa Maria, CA.). Prior to assays, the bacteria were resuspended in 2 ml of Hanks' balanced salt solution (HBSS) (Cellgro, Manassas, VA) and passed through a 20-gauge needle 5 times to break cell aggregates. The suspension was allowed to rest for 2 min at room temperature, and only the top 1 ml was ultimately used. An optical density of 0.084 at 600 nm (7×10^7 CFU/ml) was used to quantify bacterial concentrations.

Cell culture. HEp-2 cells (CCL-23) and BEAS-2B cells (CRL-9609) were obtained from the American Type Culture Collection (Manassas, VA). HEp-2 cells were grown in RPMI 1640 (Lonza, Allendale, NJ) supplemented with 10% fetal bovine serum (FBS) (Gemini Bio-products, Sacramento, CA) at 37°C and 5% CO_2. BEAS-2B cells were grown in bronchial epithelial basal medium (BEBM) supplemented with bronchial epithelial growth medium (BEGM) SingleQuot kit supplement and growth factors (CC-3170; Lonza, Allendale, NJ). For all the assays, epithelial cells were used at 80% confluence.

Microscopy. For scanning electron microscopy, HEp-2 cells were grown on coverslips placed in 24-well tissue culture plates. Bacteria were added at a multiplicity of infection (MOI) of 10. At each time point, the medium was gently removed using a Pasteur pipette, and 4% glutaraldehyde–2% paraformaldehyde (Alfa Aesar, Ward Hill, MA) was added and left for 1 h at room temperature. The coverslips were then washed three times with HBSS, treated with 1% osmium tetroxide in 0.2 M cacodylate buffer (Ted Pella Inc., Redding, CA), and dehydrated with graded solutions of acetone at room temperature. Samples were sputter coated with 15- to 20-nm gold-palladium. Micrographs were taken using the FEI Quant 600F FE scanning electron microscope at the Oregon State University Electron Microscopy Facility. Micrographs are representative of four biological experiments, and at least 30 fields were taken at each time point.

For confocal microscopy studies, HEp-2 cells were seeded and infected in 8-chamber slides at an MOI of 10. The infected monolayer was washed three times with HBSS and fixed using ice-cold methanol at −20°C for 15 min. Monolayers were blocked with 2% bovine serum albumin (BSA) (Sigma, St. Louis, MO) for 1 h. Monolayers were then incubated for 1 h at room temperature with mouse antivimentin V9 antibody (Sigma) at a dilution of 1:200 in PBST buffer (3.2 mM Na_2HPO_4, 0.5 mM KH_2PO_4, 1.3 mM KCl, 135 mM NaCl, 0.05% Tween 20, pH 7.4) and subsequently incubated with mouse IgG linked to Alexa Fluor 680 secondary antibody (1:200; Santa Cruz Biotechnology, Dallas, TX) for 30 min. For confocal microscopy, samples were examined with a Leica Zeiss LSM510 META with Axiovert 200 motorized microscope with version 3.2 LSM software. Images were acquired with the same optimized parameters for all experiments. For immunofluorescence, a Leica DM4000B microscope was used. Confocal microscopy studies were repeated three times, and over 10 fields were captured for each condition. The LSM image browser was used to analyze the images.

Formation and isolation of microaggregates. HEp-2 cells were grown in 75-cm^2 flasks (BD Biosciences, San Jose, CA), treated with 5 μg/ml of cytochalasin B (Sigma) for 2 h, and then washed three times with HBSS. A single-cell suspension of *M. avium* subsp. *hominissuis* was prepared as described above, diluted in RPMI 1640 for an MOI of 100, and incubated with HEp-2 cells at 37°C with 5% CO_2 for 24 h. The supernatant was then recovered and immediately placed on ice. Additionally, the HEp-2 cells were washed three times with ice-cold HBSS to obtain remaining microaggregates. The microaggregate suspension was then observed under a microscope for confirmation of the structure. The total supernatant was then centrifuged for 15 min at 16,000 × *g* at 4°C. The supernatant was decanted, and the pellet was resuspended in 5 ml of HBSS and centrifuged for 5 min at 150 × *g* to remove any host cells. The supernatant was then transferred to a new 50-ml conical tube and centrifuged again for 15 min at 16,000 × *g* at 4°C. The supernatant was again decanted and the pellet resuspended in 2 ml of HBSS, and the bacterial concentration was measured using optical density. For CFU determination, the bacterial inoculum was serially diluted and plated onto 7H10 agar plates.

Replication during microaggregate formation. Microaggregates were formed as described above in 75-cm^2 flasks with HEp-2 cells at 37°C with 5% CO_2 for 24 h. CFU were quantified in the initial inoculum and after 24 h by plating the suspensions onto Middlebrook 7H10 agar plates.

Bacterial RNA extraction and purification. Microaggregates were isolated as described above. All solutions used in the RNA extraction protocol were chilled on ice prior to use, and centrifugations were carried out at 4°C at 16,000 × *g* for 10 min, unless otherwise noted. The bacterial suspension was pelleted at 4°C and resuspended with 0.7 ml of RNA detergent (500 mM sodium acetate [pH 4] [Sigma], 1% Triton X-100 [Sigma], and 0.6% sodium dodecyl sulfate [Sigma]) in nuclease-free water (Ambion, Austin, TX) and 0.6 ml of acid phenol (Sigma) and transferred to a bead beater tube with 300 μl of 0.1-mm glass beads (Sigma). The bacteria were disrupted with a bead beater 6 times at maximum speed for 20 s, allowing each sample to chill between bead beater treatments. The tubes were then centrifuged for 5 min, and the upper aqueous phase was carefully transferred to a clean 1.5-ml Eppendorf tube; 0.2 ml of RNA detergent and 0.6 ml of chilled acid phenol were then added to each sample and vortexed. The same procedure was repeated, and the upper aqueous phase was again carefully transferred to a clean tube, where an additional 0.6 ml of acid phenol was added to each sample. The same procedure was repeated, and the upper aqueous layer was transferred to a clean tube and 0.6 ml of chloroform-isoamyl alcohol (25:1) (Sigma) was added. The same procedure was repeated again, and the aqueous layer was split into two tubes per sample and underwent an ethanol precipitation. Four volumes of 95% to 100% ethanol (Sigma) was added to each tube. The tubes were vortexed in a bead beater for 10 s and incubated for 30 min at −20°C. The samples were centrifuged and the supernatant removed. The pellet was resuspended with 1 ml of 75% ethanol, agitated, and centrifuged. The supernatant was removed, and the pellet was resuspended in 100% ethanol. The sample was centrifuged, and the supernatant was removed, spun a second time, and allowed to sit at 4°C to remove any excess ethanol. The pellet was then resuspended in 0.2 ml of nuclease-free water, and corresponding samples were combined. Samples were treated with recombinant DNase I (Roche, Indianapolis, IN) and RNaseOUT recombinant RNase inhibitor (Invitrogen, Carlsbad, CA) as per the manufacturer's protocol. One milliliter of TRIzol reagent (Invitrogen, Carlsbad, CA) and 0.2 ml of chloroform (Sigma) were added to each sample, and the tubes were vortexed with a beadless bead beater for 5 s. The samples were then centrifuged, the upper aqueous phase was transferred to a clean tube, and 0.6 ml of chloroform-isoamyl alcohol (24:1) (Sigma) was added to each sample. Each sample was then agitated, followed by centrifugation at 4°C and 3,000 × *g* for 10 min. The samples were then split into two tubes again and underwent a second ethanol precipitation, as described above. The pellet was resuspended in 15 μl of TE buffer (10 mM Tris-HCl and 1 mM EDTA), and corresponding samples were combined. The MICROBEnrich kit (Ambion, Austin, TX) was used according to the manufacturer's protocol on each sample to remove mammalian RNA. The final purified samples were resuspended in 5 μl of nuclease-free water. The purified bacterial RNA samples were amplified and biotin labeled using the MessageAmp II-Bacteria kit according to the manufacturer's instructions (Ambion, Austin, TX). Samples were eluted in nuclease-free water and vacuum centrifuged to a final concentration of 1 μg/ml. The concentration, quality, and purity of bacterial RNA were then checked using a NanoDrop 2000 instrument (Thermo Scientific, Wilmington, DE) as well as by electrophoresis on a DNA gel.

DNA microarrays. The amplified RNA (aRNA) was bioanalyzed and fragmented at the Center for Genome Research and Biocomputing (CGRB) at Oregon State University. The aRNA was hybridized to an *M. avium* subsp. *hominissuis*-specific microarray chip (Affymetrix, Santa Clara, CA) (25). Three biological replicates were analyzed for microaggregate and control samples. The quality of microarray hybridization was determined using the Affymetrix MAS5 algorithm, and normalization was performed by using the average of all data points for each array. Changes in expression levels were calculated by using normalized intensities and were given as ratios. Affymetrix gene chip data were extracted, normalized, and $\log_2$ transformed, and expression differences were analyzed using ArrayStar5 (DNASTAR, Madison, WI). Genes with differential fold expression intensity of ≥2 were analyzed and ranked according to fold expression.

Real-time PCR. Four genes identified as differentially expressed in the microarray were validated using relative quantitative real-time PCR with a Bio-Rad iCycler and SYBR green technology (Bio-Rad, Hercules, CA), as previously described (26). The following primers were designed based on a BLAST search of the NCBI database: MBP-1 (226 bp; forward, 5′-GTC GGA CAA GAG CGG TCC CGA GGA GGC C-3′; reverse, 5′-GTT CGG CCT TCT GGC GAG CCT CGT TGA TC-3′), MAV_5199 (135 bp; forward, 5′-GTG ACA ACA AAA GCC ATG ATC TTC TCC TG-3′; reverse, 5′-CTA TCC GAA ATC CGT TTC GTC CCG ATC CG-3′), MAV_1799 (111 bp; forward, 5′-GGA TCT GCG CCG TAC GCG TGG TGC TTG G-3′, reverse, 5′-CCA TTA GTC GTA CCG ATC ATG GCG TTG-3′), and MAV_0831 (128 bp; forward, 5′-GTG ACC GAC GAA GAC GAA TGG CGC GCC-3′, reverse, 5′-CAC TCA TAG CGT GCG TCC TCC CGG TCG C-3′). Briefly, bacterial RNA was transcribed to cDNA using SuperScript III Supermix (Invitrogen, Carlsbad, CA), according to the manufacturer's protocol. Afterwards, cDNA was denatured for 5 min at 95°C, followed by 30 cycles of amplification. Each cycle had a denaturation step of 95°C for 30 s, annealing at 60°C for 30 s, and primer extension at 68°C for 1 min. Target genes from the control and experimental groups were normalized to the expression level of the 16S RNA gene. To determine the change (*n*-fold) in gene expression, the following formula was used: change (*n*-fold) = $2^{-\Delta(\Delta C_T)}$, where ΔC_T equals C_T (target) − C_T (16S RNA) and $\Delta(\Delta C_T)$ is ΔC_T (experimental) − ΔC_T (control). Results represent the average of two technical replicates and are representative of three biological replicates.

To quantify the expression of MBP-1 during microaggregate formation by the clinical isolate MAC3388, HEp-2 cells were infected at an MOI of 10 for 24 h at 37°C with 5% CO_2. Bacterial RNA was extracted and reverse transcribed to cDNA as described above. Expression of the MBP-1 gene was then quantified by real-time PCR as described above using the primers used for microarray confirmation.

Overexpression and purification of proteins. To create an MBP-1 overexpression construct, the gene was amplified using FideliTaq PCR master mix (Affymetrix, Santa Clara, CA), and the PCR-generated fragment was fused to a red fluorescent protein (RFP) and cloned into *Escherichia coli-Mycobacterium* shuttle vector pMV261-5HRFP, encoding kanamycin resistance (27). The resulting plasmid was propagated in *E. coli* DH10B and then electroporated into *Mycobacterium smegmatis* mc^2155. Transformants were selected on 7H10 agar plates containing 100 μg/ml of kanamycin and screened by PCR using the primers originally used for PCR of the fragment.

MBP-1 protein was purified using the pET Express & Purify kit-His60 (Clontech, Mountain View, CA) as per the manufacturer's instructions and purified using His-Bind resin chromatography (Novagen, Darmstadt, Germany) as per the manufacturer's instructions. Overexpression and purification were confirmed by Western blotting using the 6XHN rabbit antibody (Clontech, Mountain View, CA).

Production and purification of antibodies. The production of antibodies was adapted from the Thermo Scientific mouse antibody production protocols (http://www.pierce-antibodies.com/custom-antibodies/mouse-antibody-production-protocols.cfm) with the following modifications. Briefly, MBP-1 protein was produced and purified as described above. Ten female C57BL/6 mice were immunized with three subcutaneous injections of 0.1 mg MBP-1 protein with incomplete Freund's adjuvant as per the manufacturer's instructions (Sigma). Boosters were given 21 and 42 days afterwards with one injection of 0.05 μg MBP-1 protein. Blood was collected at 50 days after the initial injection. Blood was centrifuged at 1,000 × *g* for 10 min, and the resulting immune serum was collected and used for experiments. The serum was tested against MBP-1 protein at a 1:5,000 dilution by Western blotting to verify specificity. Preimmunization immune serum was also examined for reactivity against MBP-1 protein. In addition, mouse anti-MBP-1 antibody and preimmunization immune serum were purified on a protein G HP Spintrap

(Thermo Scientific), which purifies the IgGs in the serum. A Bradford protein assay (Bio-Rad) was used to determine the concentration of the purified antibodies. Preimmunized serum was also obtained from mice and used as an experimental control. This study was performed according to the guidelines of and approved by the institutional animal care and use committee at Oregon State University (Animal Care and Use Proposal 4396).

Binding assay. The binding assays were carried out as previously reported (15). Briefly, HEp-2 cells were infected with *M. smegmatis* overexpressing proteins of interest at an MOI of 10 for 2 h at 4°C. To synchronize infection, cell culture plates were centrifuged for 5 min at 232 × *g* after the addition of bacteria. Wells were then washed three times with HBSS, and cells were lysed with 0.1% Triton X-100 for 15 min. Cell lysates were plated onto 7H10 agar plates supplemented with 100 μg/ml kanamycin. After growth, CFU were quantified. For the antibody blocking binding assay, microaggregates were isolated as described above and incubated with 40 μg of mouse antivimentin (V9) or nonspecific mouse IgG antibody (Sigma) and host cells at an MOI of 10. The infection was synchronized, and the cells were placed at 4°C for 2 h and processed as described above. Bacteria were plated onto 7H10 agar plates, and the number of CFU were determined. For MAV-3013-treated microaggregate binding assay, microaggregates were isolated as described above and incubated with 50 μg of purified MBP-1 or nonspecific protein for 1 h at room temperature at an MOI of 10. Microaggregates were then washed 3 times with HBSS, and HEp-2 cells were infected (synchronized), placed at 4°C for 2 h, and processed as described above. For the anti-MBP-1 immune serum binding inhibition assay, microaggregates were incubated with anti-MBP-1 immune serum diluted 1:1,000 for 1 h at room temperature and were then tested for binding to HEp-2 cells as described above. Preimmunization serum was used as a control. For binding assays performed with purified anti-MBP-1 antibody, a 1:1,000 dilution of antibody was incubated with microaggregate and planktonic bacteria for 1 h at 37°C and then tested for binding with HEp-2 cells as described above.

Western blots. For the far-Western blot, HEp-2 cells were grown in T75 flask and washed twice with HBSS. HEp-2 cells were then lysed with CelLytic M (Sigma) in the presence of protease inhibitor cocktail (Sigma), scraped off the flask, and centrifuged for 15 min at 12,000 × *g*. HEp-2 cell lysate was biotinylated using the ECL protein biotinylation module (Amersham Biosciences, Piscataway, NJ) as per the manufacturer's instructions. Biotinylated HEp-2 cell lysate was run on a 4 to 20% Mini-Protean precast SDS-PAGE protein gel (Bio-Rad) under reducing conditions and transferred to a nitrocellulose membrane (Bio-Rad). After 1 h of renaturation in 5% blocking buffer, the membrane was further incubated with 2 mg/ml of MBP-1 or nonspecific MAV_0831 protein control in protein binding buffer (100 mM NaCl, 20 mM Tris [pH 7.6], 0.5 mM EDTA, 10% glycerol, 0.1% Tween 20, 2% skim milk powder, 1 mM dithiothreitol [DTT]) overnight at 4°C with gentle shaking. On the Western blot, bound recombinant protein was detected with 6xHN polyclonal antibody (Clontech, Mountain View, CA) and streptavidin antibody (Li-Cor, Lincoln, NE) followed by the corresponding Li-Cor IR dye secondary antibodies. Host proteins that interacted with MBP-1 were subsequently excised from the protein gel using the Pierce (Rockford, IL) in-gel tryptic digestion kit and identified by mass spectrometry at the Mass Spectrometry Facility at Oregon State University.

To measure phosphorylation of HEp-2 cells by Msmeg-3013, HEp-2 cells were grown in 6-well plates overnight at 2×10^5 cells/ml and infected with Msmeg-3013 and Msmeg-empty at an MOI of 100 for 15 and 45 min at 37°C and 5% CO_2. Cells were then quickly washed twice with chilled HBSS, incubated with 100 μl of CelLytic lysis buffer (Sigma) with protease inhibitor cocktail (Sigma), and immediately scraped out of the well and put on ice. Proteins were run on SDS-polyacrylamide gels and blotted onto a nitrocellulose membrane. The membrane was then probed with anti-phosphovimentin-Ser82 antibody (MBL International, Billerica, MA) and anti-β-actin (Santa Cruz Biotechnology, Dallas, TX). Band intensities were quantified using ImageJ software. The ratio of phosphorylated vimentin compared to total protein loaded (β-actin) was determined and expressed as a proportion of the value for a mock-infected sample (set to 1).

Immunoprecipitation and pulldown assay. Rabbit antivimentin antibody (H84) (Santa Cruz Biotechnology) was cross-linked to agarose beads (Invitrogen) as per Abcam's online protocol (Abcam, Cambridge, MA). Briefly, 40 μl of agarose beads was centrifuged at 10,000 × *g* and washed once in 1× phosphate-buffered saline (PBS) (137 mM NaCl, 2.7 mM KCl, 10 mM Na_2HPO_4, and 1.8 mM KH_2PO_4). Beads were blocked in dilution buffer (1 mg/ml of BSA [Sigma] in 1× PBS) for 10 min at 4°C. The antibody solution was then prepared by adding 20 μl of 200-μg/ml antivimentin antibody (H-84) (Santa Cruz Biotechnology) to 20 μl of dilution buffer and incubated with the beads for 1 h at 4°C. Beads were then centrifuged at 10,000 × *g*, washed with 40 μl of dilution buffer, and resuspended in 40 μl of 1× PBS. To cross-link the antibody to the agarose beads, 1 ml of 13-mg/ml dimethyl pimelimidate (DMP) was mixed with 1 ml of wash buffer (0.2 M triethanolamine in 1× PBS), and the pH was adjusted to 8. Afterwards, 40 μl of the cross-linking reagent was added to the beads and rotated for 30 min at room temperature. Beads were washed in wash buffer once and incubated in DMP for a second time. This was repeated once more for a total of three cross-linking incubations and wash steps. The reaction was quenched twice in 40 μl of 50 mM ethanolamine in 1× PBS for 5 min at room temperature, and the mixture was centrifuged and aspirated. Excess antibody was removed by washing the beads twice with 1 M glycine, pH 3. Beads were then washed three times with 0.1% Triton X-100–0.1% Tween 20 buffer at room temperature. Afterwards, 40 μg of vimentin protein (Abcam, Cambridge, MA) was incubated with the antibody-agarose complex for 2 h at 4°C. The *Escherichia coli* pellet overexpressing MBP-1 was lysed by bead beater disruption of the bacterial pellet with 0.1-μm glass beads (Sigma) three times in 0.1% Triton X-100–0.1% Tween 20 buffer. The bacterial lysate was iced between bead beater treatments, centrifuged at 14,000 × *g* for 10 min, and passed through a 0.2-μm filter. The protein concentration was measured using the Bradford assay (Bio-Rad), and then 0.44 mg of bacterial lysate was incubated with 40 μl antivimentin antibody-conjugated agarose beads and control beads overnight with rotation at 4°C. Beads not treated with vimentin protein were used as a control. The protein-bead complexes were pelleted and washed three times with 150 mM NaCl and 0.1% Triton X-100. The protein-bead complexes were resuspended in Laemmli buffer (Bio-Rad) and run on a protein gel. The protein gel was transferred to a nitrocellulose membrane and probed with antivimentin (Santa Cruz Biotechnology) and anti-6xHN polyclonal antibody (Clontech).

For the pulldown assay, microaggregates were isolated as described above and biotinylated using the ECL protein biotinylation module as per the manufacturer's instructions (Amersham Biosciences). Briefly, excess biotin in the biotinylated microaggregates was quenched with 100 mM glycine and washed 3 times with 1× PBS. The bacterial pellet was then resuspended in 500 μl of 0.1% Triton–0.1% Tween, disrupted with a bead beater three times, and then purified using a Sephadex G25 column. MBP-1 protein was overexpressed and immobilized using the pET Express & Purify kit-His60 as described above. Prior to the elution step, biotinylated proteins were incubated with immobilized MBP-1 on the nickel column overnight at 4°C. The nickel column was washed with 10 ml of wash buffer and eluted in 5 ml of elution buffer. The eluate was concentrated to 100 μl using a Microsep centrifugal device (Pall, Port Washington, NY). Proteins were run on an SDS-polyacrylamide gel and blotted onto a nitrocellulose membrane. The membrane was then probed with streptavidin antibody (Li-Cor) followed by the corresponding Li-Cor IR dye secondary antibody. Bacterial proteins that interacted with MBP-1 were subsequently excised from the SDS-PAGE protein gel using the Pierce (Rockford, IL) in-gel tryptic digestion kit and identified by mass spectrometry at the Mass Spectrometry Facility at Oregon State University.

Mycobacterial 2-hybrid system (M-PFC). The mycobacterial 2-hybrid system (mycobacterial protein fragment complementation [M-

PFC]) was used out as previously described (28, 29). Vectors pUAB300 (prey) and pUAB400 (bait) were donated from the Steyn lab. As described previously (29), the MBP-1, MAV_4504, MAV_0623, and MAV_2921 genes were amplified using FideliTaq PCR master mix (Affymetrix). MBP-1 and MAV_2922 were cloned into the bait vector (pUAB400), while MAV_4504 and MAV_0623 were cloned into the prey vector (pUAB300). The resulting plasmids were propagated in *E. coli* DH10B, and then the MBP-1-pUAB400 construct was electroporated into *Mycobacterium smegmatis* mc^2155. Transformants were selected on 7H10 agar plates containing 40 μg/ml of kanamycin and screened by PCR using the primers originally used for PCR of the fragment. Bait plasmids were cultured and purified according to the manufacturer's protocols (Qiagen, Alameda, CA). The bacterial cultures were electroporated with 500 ng of bait plasmids and plated on 7H10 plates supplemented with 40 μg/ml kanamycin, 50 μg/ml hygromycin, and 20 μg/ml trimethoprim. Cultures were grown for 7 days at 37°C. Resistant colonies were restreaked onto new triple-selective plates, and plasmids were confirmed using PCR to eliminate false-positive results.

Statistical analysis. The experiments described in this paper were repeated at least two times, and data shown are means from those replicates ± standard error. When comparing two groups, the Student *t* test was used, and when analyzing more than two groups, an analysis of variance (ANOVA) was carried out. Differences between experimental and control groups were considered significant when the *P* value was <0.05. Graph Pad Prism version 5.0 software was used for statistical analysis.

Mouse infection. Female C57BL/6 mice, 6 weeks old, were infected intranasally with 20 μl of 2×10^{10} CFU per ml of microaggregates incubated with 50 μl anti-MBP-1 immune serum for 1 h at 37°C. An equal volume of preimmunization serum was used as a control. After 24 h, the mice were sacrificed and lungs were homogenized and plated onto 7H10 Middlebrook agar plates for determination of colony counts. Ten mice were used in each experimental group. This study was performed according to the guidelines of and approved by the institutional animal care and use committee at Oregon State University (Animal Care and Use Proposal 4396).

Microarray data accession number. The microarray data have been deposited in Gene Expression Omnibus (GEO) under accession number GSE55010.

RESULTS

Visualization of microaggregate formation through scanning electron microscopy. Yamazaki et al. have shown that during initial colonization of the airways, *M. avium* subsp. *hominissuis* forms microaggregates on BEAS-2B human epithelial cells, usually preceding the invasion of the mucosal surface (8). The invasive microaggregate phenotype was confirmed *in vivo* in a mycobacterial lung infection model in C57BL/6 mice. Mice were infected intranasally with equal concentrations of microaggregate and planktonic MAC104 for 24 h. Mice infected with microaggregates carried a significantly higher bacterial burden than mice infected with planktonic bacteria (Fig. 1A).

To identify the timeline of *M. avium* subsp. *hominissuis* microaggregate assembly on respiratory epithelial cells, scanning electron microscopy was carried out to follow microaggregate formation at 4, 24, and 48 h postexposure (Fig. 1B to E). Bacteria began attaching to the surface of the epithelial cell at 2 h (Fig. 1C). The formation of microaggregates was first seen at 24 h postinfection and progressed in a time-dependent manner (Fig. 1D). Although the previous study utilized BEAS-2B epithelial cells for the formation of microaggregates, for the rest of our studies HEp-2 respiratory epithelial cells were used. We have shown that *M. avium* subsp. *hominissuis* forms microaggregates on both HEp-2 and BEAS-2B respiratory epithelial cells in a similar manner (data not shown) (8). To determine whether microaggregate formation was due to bacterial replication, bacterial counts were taken at time zero and at 24 h after addition to HEp-2 epithelial cells. The results indicate that although there was a very small increase in bacterial counts, it cannot account for the total amount of bacteria in aggregates (Fig. 1F). These data agree with previously published data showing that *M. avium* subsp. *hominissuis* replicates poorly in RPMI 1640 medium (30). In addition, *M. avium* subsp. *hominissuis* has a long doubling time in medium (~12 to 18 h), which supports the conclusion that bacteria are binding together to form the microaggregates, independent of replication.

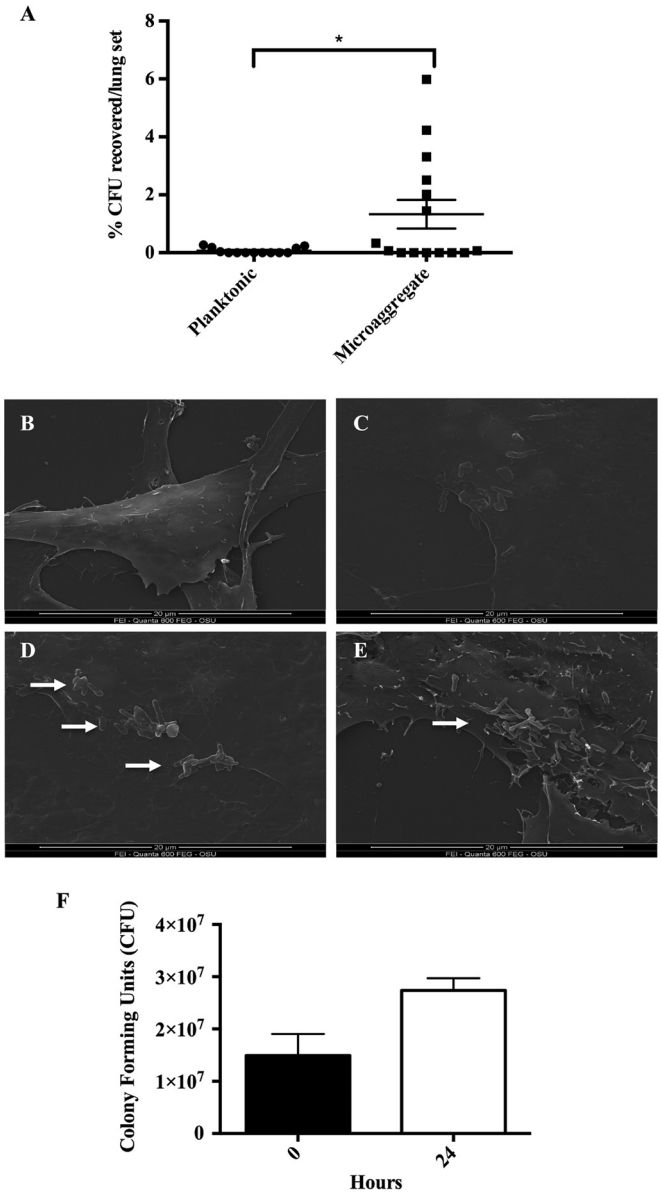

FIG 1 *In vivo* and *in vitro* characterization of microaggregates. (A) C57BL/6 mice were infected intranasally with equal concentrations of microaggregate and planktonic MAC104 for 1 day. Mice were sacrificed, and lungs were homogenized and plated on 7H10 plates for enumeration. (B to E) Micrographs taken with no infection (B) and at 4 h (C), 24 h (D), and 48 h (E) postinfection. At 48 h postinfection, bacteria are surrounded by filopodium-like protrusions on the surface of the epithelial cell. (F) Bacterial counts were taken prior to and 24 h after incubation with HEp-2 cells. *, $P < 0.05$.

Identification of differentially expressed genes during microaggregate formation. To examine the gene expression of *M. avium* subsp. *hominissuis* during microaggregate formation, a genome-wide custom microarray (Affymetrix) was used. The transcriptome of *M. avium* subsp. *hominissuis* microaggregates was compared to that of planktonic *M. avium* subsp. *hominissuis* (bacteria incubated in cell culture medium) at 24 h. Gene expression with a 2-fold difference or greater was considered relevant. Genes differentially expressed included 137 genes that had their expression level increased and 186 genes that were less expressed in microaggregates compared to planktonic *M. avium* subsp. *hominissuis*, and genes upregulated in microaggregates are listed in Table S1 in the supplemental material. Many genes encoding small hypothetical proteins were highly expressed (see Table S1 in the supplemental material). Mce genes, which have been shown to be correlated with virulence in mycobacteria, were upregulated as well (see Fig. S1 in the supplemental material). Ten percent of the genes that were upregulated 3- to 4-fold encode cell envelope proteins (see Fig. S1). MAV_3013 (henceforth called MBP-1), a hypothetical protein, with the greatest change in expression upon aggregate formation, was selected for further characterization. To examine whether MBP-1 was upregulated in a lung isolate of *M. avium* subsp. *hominissuis*, MBP-1 gene expression in strain MAC3388 was quantified during microaggregate formation. Consistent with MBP-1 expression in MAC104, there was a 2.8-fold upregulation of MBP-1 in strain MAC3388 during microaggregate formation. The microarray results were confirmed by carrying out quantitative real-time PCR (RT-PCR) for four genes, and the results showed fold changes similar to those obtained with the DNA microarray (see Table S2 in the supplemental material).

***In silico* characterization of MBP-1.** Due to the high expression profile during microaggregate formation, microaggregate-binding protein 1 (MBP-1) was selected for further characterization. Because this protein has been classified as a hypothetical protein, we initially looked for conserved domains or motifs that would suggest possible function. By analyzing the gene sequence using the Kyoto Encyclopedia of Genes and Genomes (KEGG) database, we determined that MBP-1, a 77-amino-acid protein, shared sequence similarity with the human cytoskeletal afadin- and alpha-actinin-binding protein (ADIP) and the ATP synthase E chain (see Fig. S2 in the supplemental material). MBP-1 also has four paralogs, MAV_3734, MAV_4077, MAV_1589, and MAV_1300. MAV_3734 and MAV_4077, which share the most sequence identity with MBP-1, were also upregulated during microaggregate formation. MBP-1 does not seem to be part of an operon, based on the orientation of the gene and because the genes surrounding MBP-1 are also not upregulated in the microarray. The bioinformatic program Softberry suggests that MBP-1 is located in the outer membrane of the bacteria by combining several methods of protein localization prediction, such as direct comparison with bases of homologous proteins of known localization, signal peptides, and transmembrane segments.

Functional characterization of MBP-1. To gain insight into the function of MBP-1, the protein was overexpressed in *Mycobacterium smegmatis* mc^2155, a fast-growing mycobacterium that is not able to invade epithelial cells. Although a knockout of the MBP-1 gene would be a definitive test to investigate the role of this protein during microaggregate formation, we were unable to construct a knockout due to the technical difficulty of creating a targeted mutant of a small gene without having a polarizing effect on neighboring genes. We felt that nonpathogenic *Mycobacterium smegmatis* overexpressing the full-length and mutated version of MBP-1 would serve as an adequate substitute. *Mycobacterium smegmatis* also encodes a protein, MSEMG_1170, that has 67% protein similarity to MBP-1; these two proteins do not share the ADIP and ATP synthase A protein domains when analyzed by using KEGG. In addition, the Msmeg-empty control negates any contribution of the endogenous MSMEG_1170 protein to the assays performed in this study. The ability of *M. smegmatis* overexpressing MBP-1 (Msmeg-3013) to bind or invade epithelial cells was assessed. For the binding assay, Msmeg-3013 was added to a confluent monolayer of HEp-2 cells and left for 2 h at 4°C (to prevent internalization of the bacterium). Msmeg-3013 binding to the host cells was significantly increased compared to that of *M. smegmatis* containing the empty vector (Msmeg-empty) (Fig. 2A). To determine which sequence of MBP-1 was important for binding during infection, we selected a region in the ADIP domain in MBP-1 that was conserved among human, rat, and mouse and overexpressed a dominant-negative deletion mutant of MBP-1 with deletions in this conserved region corresponding to amino acids 45 to 63 in *M. smegmatis* (Msmeg-3013Δ45-63) (see Fig. S2 in the supplemental material). Expression of Msmeg-3013Δ45-63 impaired the ability of *M. smegmatis* to bind to epithelial cells (Fig. 2A) compared with that of Msmeg-3013. To identify whether this protein plays an additional role in subsequent invasion of epithelial cells, an invasion assay was performed, but no significant differences were noted (data not shown).

Due to its role in binding to epithelial cells, we hypothesized that MBP-1 may either be transported extracellularly or be membrane bound on the surface of the bacterium. In order to determine if purified MBP-1 binds to the bacterial surface, purified MBP-1 protein was incubated with *M. avium* subsp. *hominissuis* microaggregates and with planktonic bacteria for 1 h and washed, and the binding to epithelial cells was assessed. After 2 h, microaggregates incubated with MBP-1 were able to bind to HEp-2 cells significantly better than the microaggregates treated with nonspecific protein or HBSS (Fig. 2B). Regardless of their treatment, planktonic bacteria did not show any significant differences in binding to HEp-2 cells (data not shown). These data suggest that MBP-1 probably binds to another bacterial protein, increasing the ability of microaggregates to bind the surface of epithelial cells.

To further define the role of MBP-1 during binding, we produced an antibody specifically against MBP-1 in mice (see Fig. S3 in the supplemental material). Anti-MBP-1 immune serum was used to assess the ability of the MBP-1 immune serum to block binding of microaggregates to epithelial cells. Preimmunization serum was used as a serum control. Microaggregates were incubated with anti-MBP-1 immune serum for 1 h, and the binding to HEp-2 cells was assessed. Incubation with anti-MBP-1 immune serum inhibited 40% of *M. avium* subsp. *hominissuis* binding to the host, showing the importance of MBP-1 during infection (Fig. 2C).

To demonstrate that the effect of the anti-MBP-1 immune serum was due to anti-MBP-1 antibody, IgGs were purified using protein G affinity chromatography and the antibody concentration was measured. A 0.26-mg amount of purified antibody was incubated with microaggregates for 1 h, and binding was assessed. When microaggregates were incubated with anti-MBP-1 purified antibody, microaggregate binding was significantly reduced, whereas the antibody had no effect on planktonic MAC104 bind-

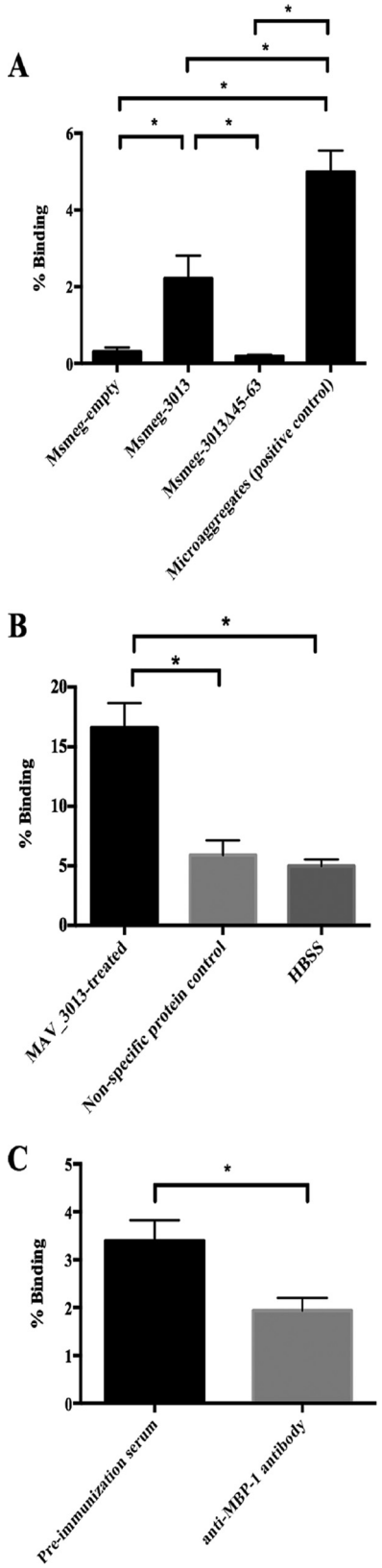

FIG 2 (A) MBP-1-overexpressing *M. smegmatis* (Msmeg-3013) has increased binding to HEp-2 cells compared to *M. smegmatis* overexpressing vector alone (Msmeg-empty). Msmeg-3013Δ45-63 has abrogated binding to host cells. The bacteria were allowed to bind to HEp-2 cells for 30 min at 4°C. Nonbound bacteria were washed, and HEp-2 cells were lysed and plated for CFU. CFU recovered were divided by the inoculum to calculate percent binding. *M. avium* subsp. *hominissuis* microaggregates were used as a positive control ($n = 9$). (B) *M. avium* subsp. *hominissuis* microaggregates pretreated with recombinant MBP-1 protein bound significantly better to HEp-2 cells than microaggregates treated with nonspecific protein or HBSS. *M. avium* subsp. *hominissuis* microaggregates were incubated with the treatment for 1 h, washed, and allowed to bind to HEp-2 cells for 2 h at 4°C. The nonspecific protein was purified Rv3354, a mycobacterial protein. Nonbound bacteria were washed, and HEp-2 cells were lysed and plated for CFU ($n = 3$). (C) Anti-MBP-1 serum significantly decreased microaggregate binding to HEp-2 cells compared to preimmunization serum. Microaggregates were incubated with anti-MBP-1 serum or preimmunization serum (negative control) for 1 h at room temperature and allowed to bind to HEp-2 cells for 2 h at 4°C ($n = 3$). For all experiments, CFU recovered were divided by the inoculum to calculate percent binding. *, $P < 0.05$.

TABLE 1 Interaction between MBP-1 and MAV_4504 or MAV_0623 in a mycobacterial 2-hybrid system

	Growth on triple-selection plates with pUAB400		
pUAB300	Empty	MBP-1	MAV_2921
Empty	Negative		
MAV_4505		Positive	
MAV_0623		Positive	
MAV_2922			Positive

ing to HEp-2 cells, similarly to the anti-MBP-1 immune serum (data not shown).

MBP-1 interacts with mycobacterial proteins MAV_4504 and MAV_0623. To identify whether MBP-1 interacts with other mycobacterial proteins on the bacterial surface during microaggregate formation, we performed a pulldown using purified MBP-1 protein as bait and *M. avium* subsp. *hominissuis* bacterial lysate as prey. Proteins recovered from the pulldown were sequenced, identified by mass spectrometry, and analyzed using the KEGG database. We found MAV_4504, an ABC transporter ATP-binding protein, and MAV_0623, a MaoC-like domain-containing protein, and confirmed the results using the mycobacterial 2-hybrid system (Table 1; Fig. 3). MAV_4504 was previously identified to be surface exposed during exponential growth phase in 7H9 medium, suggesting that MAV_4504 in its role as a transporter may be responsible for translocating or anchoring MBP-1 protein to the surface of the bacterium during microaggregate formation (29). MAV_4504 has homology to *Mycobacterium tuberculosis* H37Rv protein Rv0655, an ABC transporter, which has been shown to be present on the membrane fraction of *M. tuberculosis* and required for growth in C57BL/6J mice, suggesting that this protein plays an important role in virulence (31, 32). MAV_0623 is a probable dehydrogenase with homology to Rv3538. This protein is predicted to be involved in lipid catabolism in *Mycobacterium tuberculosis*. Rv3538 was identified by mass spectrometry to be present in whole-cell lysates but not in the culture filtrate or membrane protein fraction, indicating that MAV_0623 may interact with MBP-1 prior to being exported to the surface of the bacterium. Upon microaggregate formation, the MAV_4504 and MAV_0623 genes were not upregulated, suggesting that these proteins may be already present in the bacteria.

MBP-1 utilizes the host cytoskeletal protein vimentin during microaggregate formation. Because MBP-1 has homology to the eukaryotic protein ADIP, we hypothesized that it might interact

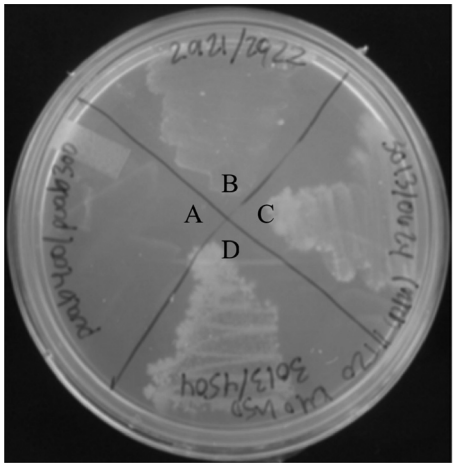

FIG 3 Interaction between MBP-1 and MAV_4504 or MAV_0623 in a mycobacterial 2-hybrid system. Growth of *M. smegmatis* harboring dual plasmids pUAB400 and pUAB300 (negative control) (A), MAV_2921-pUAB400 and MAV_2922-pUAB300 (positive control) (B), MBP-1-pUAB400 and MAV_0623-pUAB300 (C), or MBP-1-pUAB400 and MAV_4504-pUAB300 (D) on triple-selective medium (kanamycin, hygromycin, and trimethoprim) is shown. Positive protein interactions encode trimethoprim resistance. Resistant colonies were restreaked onto fresh triple-selective plates to eliminate false-positive results.

with host cell proteins. To identify them, HEp-2 cell lysate was collected and far-Western blotting was carried out with purified MBP-1 protein and purified MAV_0831 protein as a nonspecific negative control. Vimentin (P08670) was identified (Fig. 4A), and MBP-1–vimentin interaction was further confirmed through coimmunoprecipitation (Fig. 4B).

Vimentin has been used as a receptor for binding and invasion by various pathogens, such as cowpea mosaic virus (CPMV), poliovirus, Theiler's murine encephalomyelitis virus (TMEV), porcine reproductive and respiratory syndrome virus (PRRSV), *Escherichia coli* K9, group A streptococci (GAS), and *Salmonella* (33–39). To study the role of vimentin during microaggregate binding, we examined whether bacterial binding would be inhibited by blocking surface vimentin. Antivimentin monoclonal antibody V9 was incubated with bacteria and host cells to prevent bacterial access to HEp-2 surface vimentin. Treatment with antivimentin antibody significantly inhibited binding of microaggregates to HEp-2 cells, confirming the importance of MBP-1 and vimentin during microaggregate binding on epithelial cells (Fig. 4C).

MBP-1 overexpression and microaggregate formation induce changes in the host protein vimentin. Vimentin has proven to be important for invasion and binding of viruses and bacteria to epithelial cells, and for several of these pathogens, there is a notable clustering or polymerization of vimentin at the site of entry (16, 33–39). Since MBP-1 binds to vimentin, we examined the ability of MBP-1 and *M. avium* subsp. *hominissuis* microaggregates to induce vimentin polymerization using confocal microscopy. During Msmeg-3013 infection of HEp-2 cells, a significant number of bacteria colocalized with polymerized vimentin, which was absent during infection with Msmeg-empty (Fig. 5A and B). *M. avium* subsp. *hominissuis* microaggregates also induced polymerization of vimentin adjacent to the bacteria, in contrast to the planktonic bacteria (Fig. 5A and B).

The phosphorylation state of proteins is very important in the function of cytoskeletal proteins such as intermediate filaments. Previous studies have illustrated that during infection, African swine fever virus (ASFV) infection and *E. coli* K9 infection induce phosphorylation of the N-terminal domain of vimentin on Ser82 (16, 40). Since overexpression of MBP-1 induced polymerization of vimentin, we examined whether vimentin (Ser82) phosphorylation was induced during Msmeg-3013 infection of epithelial cells. Infection of HEp-2 cells with Msmeg-3013 increased the amount of phosphorylated vimentin compared to that with Msmeg-empty, (Fig. 5C and D).

***In vivo* antibody inhibition assay.** The *in vitro* data suggest that MBP-1 protein is a major component of microaggregate binding to epithelial cells, and binding was inhibited by anti-MBP-1 immune serum *in vitro*. To test the importance of MBP-1 *in vivo*, two groups of 10 female C57BL/6 mice were infected intranasally with microaggregates that had been incubated with 50 μl of anti-MBP-1 immune serum or preimmunization serum for 1 h at 37°C. Mice were sacrificed after 24 h, and lungs were plated to enumerate bacterial colonization. Mice that were infected with microaggregates incubated with anti-MBP-1 immune serum provided significant protection against colonization compared to microaggregates incubated with preimmunization serum, suggesting that MBP-1 antibody plays an important role during infection *in vivo* (Fig. 6).

DISCUSSION

In comparison to disease caused by other lung pathogens, such as *Mycobacterium tuberculosis*, nontuberculous mycobacterial lung disease has not been extensively studied. Previous studies have shown that *M. avium* subsp. *hominissuis* can successfully cross the bronchial airway mucosa after preexposure to host cells for 24 h, which is coupled with microaggregate formation on the surface of the epithelial cells. We have identified and characterized MBP-1, a protein differentially expressed upon microaggregate formation that plays a role in binding to the respiratory mucosa and is potentially a good candidate for prophylactic therapy.

MBP-1, the most highly expressed hypothetical protein, is associated with increased ability to bind respiratory epithelial cells, and serum against MBP-1 provided significant protection against infection *in vitro* and *in vivo*. The robustness of the microarray was confirmed by finding similar bacterial gene expression changes with various other pathogenic bacteria under comparable conditions (41). Studies on *Neisseria meningitidis* and *Shigella flexneri* have shown that at the onset of infection, the bacteria undergo extensive surface remodeling that is similar to what is observed during microaggregate formation, where 10% of 3- and 4-fold-upregulated genes are associated with the cellular envelope (42, 43). Six *mce* (mammalian cell entry) genes, which were shown to confer on nonpathogenic *Escherichia coli* the ability to invade and survive inside host cells, were also upregulated during microaggregate formation. Similarly to what has been described with *Burkholderia* infection, *M. avium* subsp. *hominissuis* microaggregate genes involved in bacterial growth and proliferation were downregulated (44). "Housekeeping" genes involved in protein synthesis and transcription in *Vibrio*, *Shigella*, and *Listeria* during infection of host cells were downregulated in a manner similar to that for *M. avium* subsp. *hominissuis* microaggregates (43, 45).

The ability of bacteria to shift metabolically in response to different environmental cues is very important for survival, due to

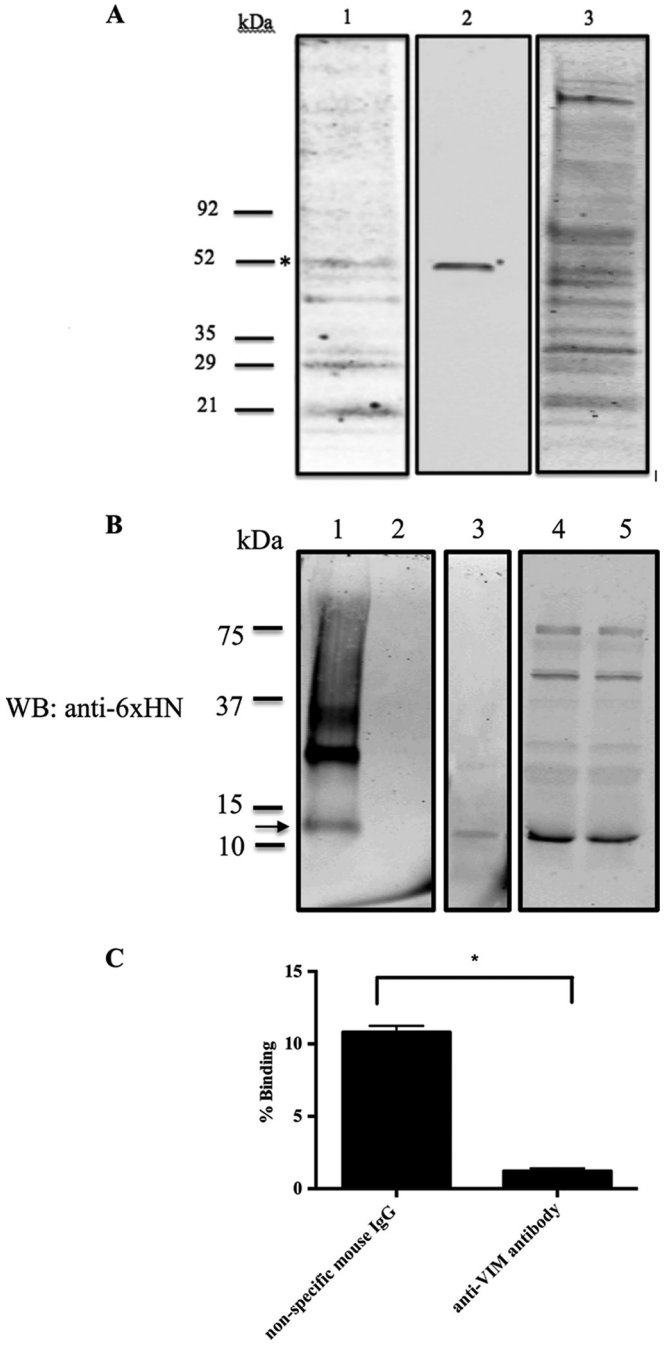

FIG 4 MBP-1 interacts with the host protein vimentin. (A) Identification of potential MBP-1 host binding partner(s) by far-Western blotting. HEp-2 protein lysate was transferred to a nitrocellulose membrane and then incubated with recombinant MBP-1 (2 mg) (lane 1), positive-control vimentin protein (lane 2), or nonspecific protein MAV_0831 (lane 3) overnight at 4°C. After washing, bound recombinant protein was detected with anti-6xHN rabbit antibody or antivimentin V9 antibody. Four bands were selected for mass spectrometry identification. *, vimentin protein band. (B) Confirmation of MBP-1 and vimentin binding through coimmunoprecipitation. Lane 1, *E. coli* lysate (13 μl) overexpressing 6xHN-tagged MBP-1 interacting with vimentin protein and antibody-conjugated agarose beads. Lanes 2 to 5, negative control (lane 2), purified MBP-1 recombinant protein (lane 3), 6xHN-tagged MBP-1 (13 μl) that was added to pull down with vimentin protein (loading control) (lane 4), and 6xHN-tagged MBP-1 (13 μl) that was added to pull down without vimentin protein (loading control) (lane 5). Beads were washed three times in 150 mM NaCl–0.1% Triton X-100 buffer and run on an SDS-polyacrylamide gel. The Western blot was then probed with anti-6xHN recombinant antibody. As a negative control, no vimentin protein was added to the vimentin antibody-conjugated agarose beads to exclude nonspecific binding. (C) *M. avium* subsp. *hominissuis* microaggregate binding to HEp-2 cells is inhibited by antivimentin antibody (V9). For antibody blocking assay, microaggregates were incubated with 40 μg of antivimentin (V9) antibody or 40 μg of nonspecific mouse IgG and host cells at the onset of infection for 2 h. *, $P < 0.05$.

limited availability of nutrients for growth inside the host. From the microarray, we can also gain insights about the metabolism of *M. avium* subsp. *hominissuis* during microaggregate formation. Although controversial, emerging evidence suggests that *M. tuberculosis* utilizes fatty acids rather than carbohydrates in the phagosome, which contrasts from other pathogenic bacteria (46–48). Catabolic beta-oxidation of fatty acid chains yields both acetyl coenzyme A (acetyl-CoA) and propionyl-CoA, where propionyl-CoA is then assimilated via the methylcitrate cycle and acetyl-CoA continues on to the citric acid cycle for energy. Furthermore, the upregulation of the methlyisocitrate lyase (*prpB*), methylcitrate synthase (*prpC*), and methylcitrate dehydratase (*prpD*) genes during microaggregate formation suggests that beta-oxidation also occurs extracellularly with the breakdown of host cell surface fatty acids.

MBP-1 has conserved domains matching the human afadin- and alpha-actinin-binding protein (ADIP). ADIP is involved in the organization of the actin cytoskeleton (49). It is located at cell-cell junctions and serves to connect the nectin-afadin and E-cadherin-catenin systems through the protein α-actinin in the host cell. *Listeria monocytogenes* expresses ActA, a bacterial protein with strong homology to the cytoskeletal protein vinculin that is involved in moving and spreading intracellularly by interacting with actin (50). By containing the ADIP domain that recognizes afadin and α-actinin, one can speculate that MBP-1 could be a product of the coevolution of mycobacteria with eukaryotic cells.

MBP-1 binds to vimentin, a type III intermediate filament that is part of the cytoskeleton, and has important roles in cell wall integrity, attachment, migration, and cell signaling (51). Bacteria and viruses can both exploit surface-exposed and cytoplasmic vimentin for adhesion and invasion of nonphagocytic cells (33, 39, 40). The *Salmonella* virulence protein SptP recruits vimentin to the membrane ruffles at the host cell wall (39). Cowpea mosaic virus (CPMV) is able to specifically invade endothelial cells via surface vimentin (33). African swine fever virus (ASFV) infection leads to vimentin-mediated cages surrounding viral particles, which are regulated by phosphorylation of the head domain Ser82 of vimentin (40). Similarly to cowpea mosaic virus and other pathogens, MBP-1 can induce the polymerization and phosphorylation of vimentin, demonstrating that *M. avium* subsp. *hominissuis* microaggregates can directly modulate the host cytoskeleton. The abrogation of the ability of microaggregates to bind to host cells when treated with antivimentin antibody strongly suggests that vimentin is a major pathway for microaggregate binding. We currently have no evidence to suggest that other mycobacterial binding proteins (FAP, Hlp, and HBHA) play an additional role in binding of microaggregates to host cells, but our results seem to indicate that binding via vimentin is a specific and major route for microaggregates. Also, since microaggregates bind more efficiently to epithelial cells than Msmeg-3013 and vimentin is the predominant route of microaggregate binding, one may infer that microaggregates express MBP-1 at higher concentrations than *M.*

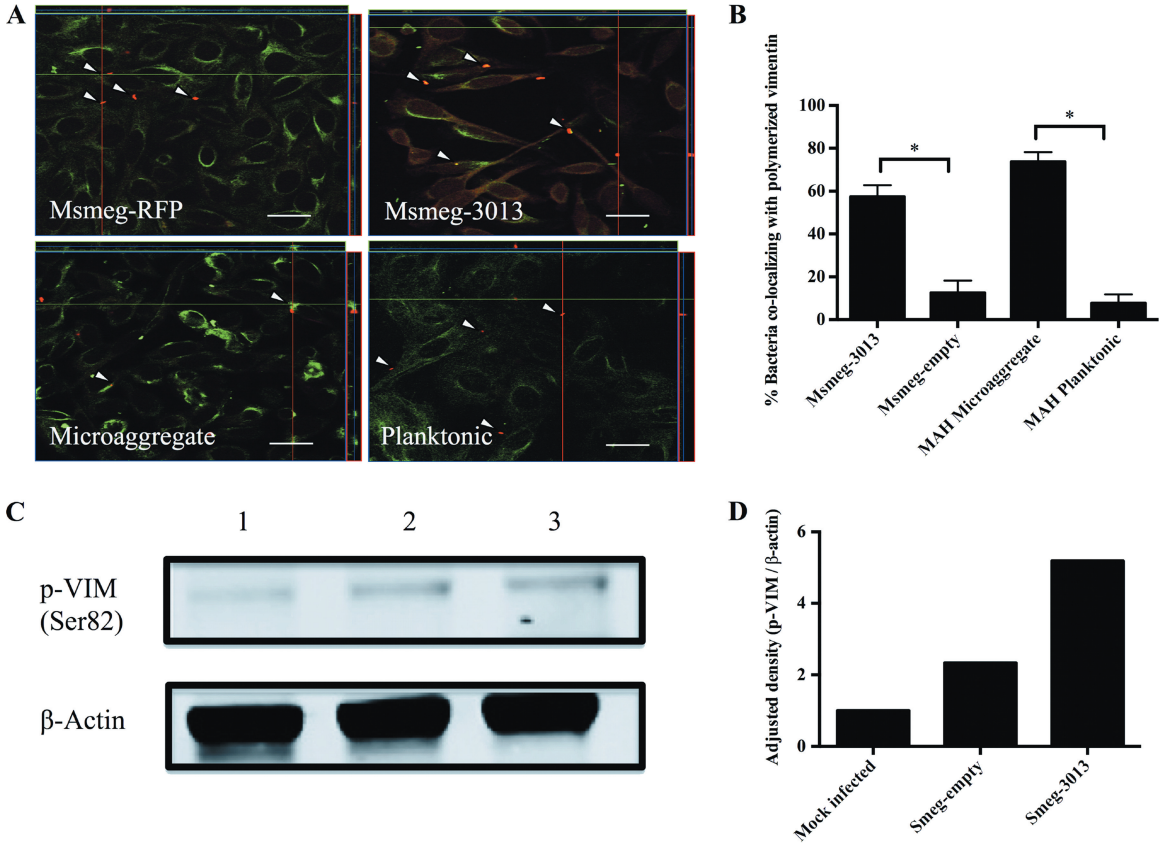

FIG 5 MBP-1 protein and *M. avium* subsp. *hominissuis* microaggregate formation stimulate vimentin polymerization in HEp-2 cells. (A) Immunofluorescence microscopy was used to examine the colocalization between vimentin polymerization, Msmeg-3013, and MAC104 microaggregates. HEp-2 cells were infected with Msmeg-RFP, Msmeg-3013, MAC104 microaggregates, or MAC104-planktonic bacteria for 2 h. Vimentin is labeled in green with mouse antivimentin (V9) antibody. Bacteria were labeled in red with TAMRA-SE prior to infection. Arrowheads indicate areas where bacteria and vimentin are colocalized. Scale bar = 20 μm. (B) Average levels of vimentin clustering were calculated from the visualization of 10 randomly selected fields for each treatment. Percentages shown represent the number of total bacteria associated with vimentin polymerization divided by the total number of bacteria. *, $P < 0.05$. (C) HEp-2 protein lysate was isolated at 45 min postinfection from uninfected cells (lane 1) or cells infected with Msmeg-empty (lane 2) or Msmeg-3013 (lane 3). Proteins were run on an SDS-PAGE protein gel and stained with antiphosphovimentin Ser82 antibody and β-actin. (D) Band intensities were quantified using ImageJ software. The ratio of phosphorylated vimentin to total protein loaded (β-actin) was determined and expressed as a proportion of the result for the mock-infected sample (set to 1). These data are for one representative of two independent replicates.

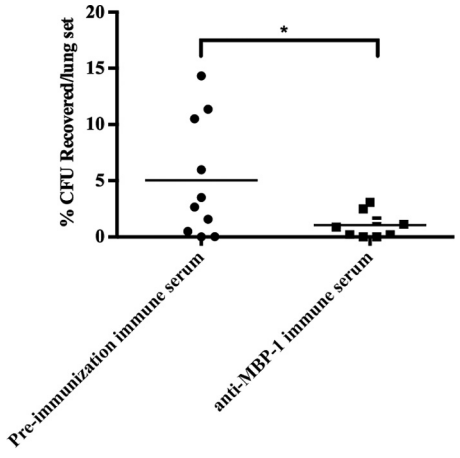

FIG 6 Anti-MBP-1 immune serum provides protection in the lungs against microaggregate infection *in vivo*. C57BL/6 mice were intranasally infected with microaggregates incubated with anti-MBP-1 immune serum or preimmunization immune serum for 1 day. Lungs were homogenized and plated on 7H10 Middlebrook agar for enumeration. *, $P < 0.05$.

smegmatis overexpressing MBP-1. There is now increasing evidence suggesting that utilization of vimentin by pathogens is a conserved mechanism for bacterial adhesion and entry into nonphagocytic host cells.

Mycobacterial lung infections appear preferentially in late-term infections in patients with cystic fibrosis, when lungs are severely damaged, and is coupled with high expression of vimentin, which plays an important role in wound healing (52). Blocking or inhibiting the interaction between vimentin and MBP-1 through prophylactic treatment with anti-MBP-1 antibody may provide significant protection against *M. avium* subsp. *hominissuis* lung infection. Our study suggests that overexpression of vimentin present in compromised lungs such as those of patients with cystic fibrosis or bronchiectasis may serve as a likely receptor for *M. avium* subsp. *hominissuis* adhesion and subsequent lung disease.

Microaggregate and biofilm formation has been described in various other pathogens and is a key component in establishing infection as well as persistence in the host (17–22). *M. avium* subsp. *hominissuis* can form robust, complex biofilms in the envi-

ronment, including urban water systems (53). When *M. avium* subsp. *hominissuis* first comes into contact with the airway epithelium, the bacteria initiate the process of microaggregation, which can lead to biofilm formation. It is unknown whether the bacterium receives signs from the host epithelial cells that stimulate microaggregation. The high frequency of reoccurrences in the lungs may indicate that biofilms play an active role during infection in patients with mycobacterial lung infections (7). Preliminary analysis of gene expression during a 7-day biofilm shows that 78/137 genes upregulated and 65/186 genes downregulated during the biofilm are correspondingly expressed during microaggregate formation (data not published). The expression of common genes has significant implications on how antibiotics are administered to patients with NTM lung infections. By identifying and blocking the crucial proteins necessary for the initiation of biofilm formation, we can reduce the bacterial burden and potentially interfere with infection.

In summary, we have identified differentially expressed proteins during microaggregate formation by *M. avium* subsp. *hominissuis*. We uncovered a novel mycobacterial binding mechanism in which MBP-1, a protein highly expressed during microaggregate formation, is used to adhere to the host epithelium by interacting with the host cytoskeletal protein vimentin. The observations described in this paper begin to define important steps of *M. avium* subsp. *hominissuis* pathogenesis in the respiratory mucosa.

ACKNOWLEDGMENTS

This work was supported by grant AI 043199 from the National Institutes of Health and by the Microbiology Foundation, San Francisco, CA.

REFERENCES

1. **Inderlied CB, Kemper CA, Bermudez LE.** 1993. The Mycobacterium avium complex. Clin Microbiol Rev **6:**266–310.
2. **Orme IM, Ordway DJ.** 2014. Host response to nontuberculous mycobacterial infections of current clinical importance. Infect Immun **82:**3516–3522. http://dx.doi.org/10.1128/IAI.01606-13.
3. **Levy I, Grisaru-Soen G, Lerner-Geva L, Kerem E, Blau H, Bentur L, Aviram M, Rivlin J, Picard E, Lavy A, Yahav Y, Rahav G.** 2008. Multicenter cross-sectional study of nontuberculous mycobacterial infections among cystic fibrosis patients, Israel. Emerg Infect Dis **14:**378–384. http://dx.doi.org/10.3201/eid1403.061405.
4. **Griffith DE, Aksamit T, Brown-Elliott BA, Catanzaro A, Daley C, Gordin F, Holland SM, Horsburgh R, Huitt G, Iademarco MF, Iseman M, Olivier K, Ruoss S, von Reyn CF, Wallace RJ, Jr, Winthrop K, ATS Mycobacterial Diseases Subcommittee, American Thoracic Society, Infectious Disease Society of America.** 2007. An official ATS/IDSA statement: diagnosis, treatment, and prevention of nontuberculous mycobacterial diseases. Am J Respir Crit Care Med **175:**367–416. http://dx.doi.org/10.1164/rccm.200604-571ST.
5. **Prince DS, Peterson DD, Steiner RM, Gottlieb JE, Scott R, Israel HL, Figueroa WG, Fish JE.** 1989. Infection with Mycobacterium avium complex in patients without predisposing conditions. N Engl J Med **321:**863–868. http://dx.doi.org/10.1056/NEJM198909283211304.
6. **Wolinsky E.** 1979. Nontuberculous mycobacteria and associated diseases. Am Rev Respir Dis **119:**107–159.
7. **Carter G, Young LS, Bermudez LE.** 2004. A subinhibitory concentration of clarithromycin inhibits Mycobacterium avium biofilm formation. Antimicrob Agents Chemother **48:**4907–4910. http://dx.doi.org/10.1128/AAC.48.12.4907-4910.2004.
8. **Yamazaki Y, Danelishvili L, Wu M, Hidaka E, Katsuyama T, Stang B, Petrofsky M, Bildfell R, Bermudez LE.** 2006. The ability to form biofilm influences Mycobacterium avium invasion and translocation of bronchial epithelial cells. Cell Microbiol **8:**806–814. http://dx.doi.org/10.1111/j.1462-5822.2005.00667.x.
9. **Voss S, Hallstrom T, Saleh M, Burchhardt G, Pribyl T, Singh B, Riesbeck K, Zipfel PF, Hammerschmidt S.** 2013. The choline-binding protein PspC of Streptococcus pneumoniae interacts with the C-terminal heparin-binding domain of vitronectin. J Biol Chem **288:**15614–15627. http://dx.doi.org/10.1074/jbc.M112.443507.
10. **Schorey JS, Holsti MA, Ratliff TL, Allen PM, Brown EJ.** 1996. Characterization of the fibronectin-attachment protein of Mycobacterium avium reveals a fibronectin-binding motif conserved among mycobacteria. Mol Microbiol **21:**321–329. http://dx.doi.org/10.1046/j.1365-2958.1996.6381353.x.
11. **Pethe K.** 2000. Characterization of the heparin-binding site of the mycobacterial heparin-binding hemagglutinin adhesin. J Biol Chem **275:**14273–14280. http://dx.doi.org/10.1074/jbc.275.19.14273.
12. **Shimoji Y, Ng V, Matsumura K, Fischetti VA, Rambukkana A.** 1999. A 21-kDa surface protein of Mycobacterium leprae binds peripheral nerve laminin-2 and mediates Schwann cell invasion. Proc Natl Acad Sci U S A **96:**9857–9862. http://dx.doi.org/10.1073/pnas.96.17.9857.
13. **Kuo CJ, Bell H, Hsieh CL, Ptak CP, Chang YF.** 2012. Novel mycobacteria antigen 85 complex binding motif on fibronectin. J Biol Chem **287:**1892–1902. http://dx.doi.org/10.1074/jbc.M111.298687.
14. **Dam T, Danelishvili L, Wu M, Bermudez LE.** 2006. The fadD2 gene is required for efficient Mycobacterium avium invasion of mucosal epithelial cells. J Infect Dis **193:**1135–1142. http://dx.doi.org/10.1086/501469.
15. **Bermudez LE, Young LS.** 1994. Factors affecting invasion of HT-29 and HEp-2 epithelial cells by organisms of the Mycobacterium avium complex. Infect Immun **62:**2021–2026.
16. **Chi F, Jong TD, Wang L, Ouyang Y, Wu C, Li W, Huang SH.** 2010. Vimentin-mediated signalling is required for IbeA+ E. coli K1 invasion of human brain microvascular endothelial cells. Biochem J **427:**79–90. http://dx.doi.org/10.1042/BJ20091097.
17. **Lepanto P, Bryant DM, Rossello J, Datta A, Mostov KE, Kierbel A.** 2011. Pseudomonas aeruginosa interacts with epithelial cells rapidly forming aggregates that are internalized by a Lyn-dependent mechanism. Cell Microbiol **13:**1212–1222. http://dx.doi.org/10.1111/j.1462-5822.2011.01611.x.
18. **Frick IM, Morgelin M, Bjorck L.** 2000. Virulent aggregates of Streptococcus pyogenes are generated by homophilic protein-protein interactions. Mol Microbiol **37:**1232–1247. http://dx.doi.org/10.1046/j.1365-2958.2000.02084.x.
19. **Sherlock O, Schembri MA, Reisner A, Klemm P.** 2004. Novel roles for the AIDA adhesin from diarrheagenic Escherichia coli: cell aggregation and biofilm formation. J Bacteriol **186:**8058–8065. http://dx.doi.org/10.1128/JB.186.23.8058-8065.2004.
20. **Menozzi FD, Boucher PE, Riveau G, Gantiez C, Locht C.** 1994. Surface-associated filamentous hemagglutinin induces autoagglutination of Bordetella pertussis. Infect Immun **62:**4261–4269.
21. **Helaine S, Carbonnelle E, Prouvensier L, Beretti JL, Nassif X, Pelicic V.** 2005. PilX, a pilus-associated protein essential for bacterial aggregation, is a key to pilus-facilitated attachment of Neisseria meningitidis to human cells. Mol Microbiol **55:**65–77. http://dx.doi.org/10.1111/j.1365-2958.2004.04372.x.
22. **Barnes AM, Ballering KS, Leibman RS, Wells CL, Dunny GM.** 2012. Enterococcus faecalis produces abundant extracellular structures containing DNA in the absence of cell lysis during early biofilm formation. mBio **3**(4):e00193-12. http://dx.doi.org/10.1128/mBio.00193-12.
23. **Kapral FA, Godwin JR, Dye ES.** 1980. Formation of intraperitoneal abscesses by Staphylococcus aureus. Infect Immun **30:**204–211.
24. **Eriksson J, Eriksson OS, Jonsson AB.** 2012. Loss of meningococcal PilU delays microcolony formation and attenuates virulence in vivo. Infect Immun **80:**2538–2547. http://dx.doi.org/10.1128/IAI.06354-11.
25. **Harriff MJ, Wu M, Kent ML, Bermudez LE.** 2008. Species of environmental mycobacteria differ in their abilities to grow in human, mouse, and carp macrophages and with regard to the presence of mycobacterial virulence genes, as observed by DNA microarray hybridization. Appl Environ Microbiol **74:**275–285. http://dx.doi.org/10.1128/AEM.01480-07.
26. **Danelishvili L, Poort MJ, Bermudez LE.** 2004. Identification of Mycobacterium avium genes up-regulated in cultured macrophages and in mice. FEMS Microbiol Lett **239:**41–49. http://dx.doi.org/10.1016/j.femsle.2004.08.014.
27. **Danelishvili L, Everman JL, McNamara MJ, Bermudez LE.** 2011. Inhibition of the plasma-membrane-associated serine protease cathepsin G by Mycobacterium tuberculosis Rv3364c suppresses caspase-1 and pyroptosis in macrophages. Front Microbiol **2:**281. http://dx.doi.org/10.3389/fmicb.2011.00281.
28. **Singh A, Mai D, Kumar A, Steyn AJ.** 2006. Dissecting virulence pathways of Mycobacterium tuberculosis through protein-protein association. Proc

Natl Acad Sci U S A **103:**11346–11351. http://dx.doi.org/10.1073/pnas.0602817103.
29. **McNamara M, Danelishvili L, Bermudez LE.** 2012. The Mycobacterium avium ESX-5 PPE protein, PPE25-MAV, interacts with an ESAT-6 family Protein, MAV_2921, and localizes to the bacterial surface. Microb Pathog **52:**227–238. http://dx.doi.org/10.1016/j.micpath.2012.01.004.
30. **Bermudez LE, Goodman J.** 1996. Mycobacterium tuberculosis invades and replicates within type II alveolar cells. Infect Immun **64:**1400–1406.
31. **Gu S, Chen J, Dobos KM, Bradbury EM, Belisle JT, Chen X.** 2003. Comprehensive proteomic profiling of the membrane constituents of a Mycobacterium tuberculosis strain. Mol Cell Proteomics **2:**1284–1296. http://dx.doi.org/10.1074/mcp.M300060-MCP200.
32. **Sassetti CM, Boyd DH, Rubin EJ.** 2003. Genes required for mycobacterial growth defined by high density mutagenesis. Mol Microbiol **48:**77–84. http://dx.doi.org/10.1046/j.1365-2958.2003.03425.x.
33. **Koudelka KJ, Destito G, Plummer EM, Trauger SA, Siuzdak G, Manchester M.** 2009. Endothelial targeting of cowpea mosaic virus (CPMV) via surface vimentin. PLoS Pathog **5:**e1000417. http://dx.doi.org/10.1371/journal.ppat.1000417.
34. **Bienz K, Egger D, Rasser Y, Bossart W.** 1983. Intracellular distribution of poliovirus proteins and the induction of virus-specific cytoplasmic structures. Virology **131:**39–48. http://dx.doi.org/10.1016/0042-6822(83)90531-7.
35. **Nedellec P, Vicart P, Laurent-Winter C, Martinat C, Prevost MC, Brahic M.** 1998. Interaction of Theiler's virus with intermediate filaments of infected cells. J Virol **72:**9553–9560.
36. **Kim JK, Fahad AM, Shanmukhappa K, Kapil S.** 2006. Defining the cellular target(s) of porcine reproductive and respiratory syndrome virus blocking monoclonal antibody 7G10. J Virol **80:**689–696. http://dx.doi.org/10.1128/JVI.80.2.689-696.2006.
37. **Zou Y, He L, Huang SH.** 2006. Identification of a surface protein on human brain microvascular endothelial cells as vimentin interacting with Escherichia coli invasion protein IbeA. Biochem Biophys Res Commun **351:**625–630. http://dx.doi.org/10.1016/j.bbrc.2006.10.091.
38. **Bryant AE, Bayer CR, Huntington JD, Stevens DL.** 2006. Group A streptococcal myonecrosis: increased vimentin expression after skeletal-muscle injury mediates the binding of Streptococcus pyogenes. J Infect Dis **193:**1685–1692. http://dx.doi.org/10.1086/504261.
39. **Murli S, Watson RO, Galan JE.** 2001. Role of tyrosine kinases and the tyrosine phosphatase SptP in the interaction of Salmonella with host cells. Cell Microbiol **3:**795–810. http://dx.doi.org/10.1046/j.1462-5822.2001.00158.x.
40. **Stefanovic S, Windsor M, Nagata KI, Inagaki M, Wileman T.** 2005. Vimentin rearrangement during African swine fever virus infection involves retrograde transport along microtubules and phosphorylation of vimentin by calcium calmodulin kinase II. J Virol **79:**11766–11775. http://dx.doi.org/10.1128/JVI.79.18.11766-11775.2005.
41. **La MV, Raoult D, Renesto P.** 2008. Regulation of whole bacterial pathogen transcription within infected hosts. FEMS Microbiol Rev **32:**440–460. http://dx.doi.org/10.1111/j.1574-6976.2008.00103.x.
42. **Grifantini R, Bartolini E, Muzzi A, Draghi M, Frigimelica E, Berger J, Ratti G, Petracca R, Galli G, Agnusdei M, Giuliani MM, Santini L, Brunelli B, Tettelin H, Rappuoli R, Randazzo F, Grandi G.** 2002. Previously unrecognized vaccine candidates against group B meningococcus identified by DNA microarrays. Nat Biotechnol **20:**914–921. http://dx.doi.org/10.1038/nbt728.
43. **Lucchini S, Liu H, Jin Q, Hinton JC, Yu J.** 2005. Transcriptional adaptation of Shigella flexneri during infection of macrophages and epithelial cells: insights into the strategies of a cytosolic bacterial pathogen. Infect Immun **73:**88–102. http://dx.doi.org/10.1128/IAI.73.1.88-102.2005.
44. **Tuanyok A, Tom M, Dunbar J, Woods DE.** 2006. Genome-wide expression analysis of Burkholderia pseudomallei infection in a hamster model of acute melioidosis. Infect Immun **74:**5465–5476. http://dx.doi.org/10.1128/IAI.00737-06.
45. **Joseph B, Przybilla K, Stuhler C, Schauer K, Slaghuis J, Fuchs TM, Goebel W.** 2006. Identification of Listeria monocytogenes genes contributing to intracellular replication by expression profiling and mutant screening. J Bacteriol **188:**556–568. http://dx.doi.org/10.1128/JB.188.2.556-568.2006.
46. **Munoz-Elias EJ, Upton AM, Cherian J, McKinney JD.** 2006. Role of the methylcitrate cycle in Mycobacterium tuberculosis metabolism, intracellular growth, and virulence. Mol Microbiol **60:**1109–1122. http://dx.doi.org/10.1111/j.1365-2958.2006.05155.x.
47. **Graham JE, Clark-Curtiss JE.** 1999. Identification of Mycobacterium tuberculosis RNAs synthesized in response to phagocytosis by human macrophages by selective capture of transcribed sequences (SCOTS). Proc Natl Acad Sci U S A **96:**11554–11559. http://dx.doi.org/10.1073/pnas.96.20.11554.
48. **Dubnau E, Smith I.** 2003. Mycobacterium tuberculosis gene expression in macrophages. Microbes Infect **5:**629–637. http://dx.doi.org/10.1016/S1286-4579(03)00090-X.
49. **Asada M, Irie K, Morimoto K, Yamada A, Ikeda W, Takeuchi M, Takai Y.** 2003. ADIP, a novel Afadin- and alpha-actinin-binding protein localized at cell-cell adherens junctions. J Biol Chem **278:**4103–4111. http://dx.doi.org/10.1074/jbc.M209832200.
50. **Domann E, Wehland J, Rohde M, Pistor S, Hartl M, Goebel W, Leimeister-Wachter M, Wuenscher M, Chakraborty T.** 1992. A novel bacterial virulence gene in Listeria monocytogenes required for host cell microfilament interaction with homology to the proline-rich region of vinculin. EMBO J **11:**1981–1990.
51. **Ivaska J, Pallari HM, Nevo J, Eriksson JE.** 2007. Novel functions of vimentin in cell adhesion, migration, and signaling. Exp Cell Res **313:**2050–2062. http://dx.doi.org/10.1016/j.yexcr.2007.03.040.
52. **Rogel MR, Soni PN, Troken JR, Sitikov A, Trejo HE, Ridge KM.** 2011. Vimentin is sufficient and required for wound repair and remodeling in alveolar epithelial cells. FASEB J **25:**3873–3883. http://dx.doi.org/10.1096/fj.10-170795.
53. **Carson LA, Petersen NJ, Favero MS, Aguero SM.** 1978. Growth characteristics of atypical mycobacteria in water and their comparative resistance to disinfectants. Appl Environ Microbiol **36:**839–846.